

A COMPUTATIONAL SCHEME FOR OPTIONS UNDER JUMP DIFFUSION PROCESSES

KAI ZHANG AND SONG WANG

Abstract. In this paper we develop two novel numerical methods for the partial integral differential equation arising from the valuation of an option whose underlying asset is governed by a jump diffusion process. These methods are based on a fitted finite volume method for the spatial discretization, an implicit-explicit time stepping scheme and the Crank-Nicolson time stepping method. We show that the discretization methods are unconditionally stable in time and the system matrices of the resulting linear systems are M -matrices. The resulting linear systems involve products of a dense matrix and vectors and an Fast Fourier Transformation (FFT) technique is used for the evaluation of these products. Furthermore, a splitting technique is proposed for the solution of the discretized system arising from the Crank-Nicolson scheme. Numerical results are presented to show the rates of convergence and the robustness of the numerical method.

Key Words. Jump diffusion processes, Option pricing, Finite volume method, Integral partial differential equation, FFT.

1. Introduction

It is well known that the assumption of log-normal stock diffusion with constant volatility in the standard Black-Scholes model of option pricing is not consistent with that of the market price movement. This phenomenon is often referred to as the volatility skew or smile [10] and exists in all the major stock index markets today. In order to capture the existence of volatility smiles, extensions of the Black-Scholes model have been proposed. Generally speaking, three approaches have been studied in the finance literature: the stochastic volatility approach [9, 11], the deterministic volatility function approach [8] and the jump diffusion model [14, 23, 5, 7]. Among them, jump diffusion, first introduced by Merton in [14], is more attractive than the other two. Contrary to the Black-Scholes model [4], the stock price in the jump diffusion model is not a continuous function of time. This allows to account for large changes in market prices due to rare events. More importantly, the jump diffusion model yields implied volatility curves similar to volatility smiles observed on markets.

Unlike the standard Black-Scholes model, the valuation of options under jump diffusion processes requires solving a partial integral differential equation. This is challenging to handle numerically since a non-local integration term is involved. There are several existing numerical methods based on the finite difference method for this problem. In [2], a method based on the multinomial trees is proposed, which is actually an explicit type finite difference approach. Hence, it is first-order accurate and conditionally stable. In [23] the author developed a method for the equation which treats the integral term explicitly and the other terms implicitly.

Received by the editors August 30, 2007 and, in revised form, December 3, 2007.
2000 *Mathematics Subject Classification.* 65M12, 65M60, 91B28.

This method is only first-order accurate and conditionally stable. In [3], an operator splitting method coupled with an FFT for the evaluation of the integral term is proposed, producing an unconditionally stable and 2nd-order accurate scheme. In [1], a second order backward difference scheme in time is developed, where the FFT technique is also used to evaluate the integral term and two operator splitting methods are proposed to solve the resulting system iteratively.

It is well known that in the case that the volatility or underlying asset price goes to zero, the Black-Scholes partial differential equation becomes convection-dominant so that solutions to the equation may display boundary or interior layers. Standard methods such as the central finite difference and piecewise linear finite element methods cannot handle this difficulty [19]. The same problem also appears in the partial integral differential equation resulting from the jump diffusion model. To overcome this difficulty, a fitted finite volume method is designed in [18, 20] to price the European and American options. The method is based on a popular exponentially fitting technique widely used for problems with boundary and interior layers (cf. [15, 16]).

In this paper, we present two discretization methods for the partial integral differential equation arising from the valuation of European vanilla options. Although the methods are presented for this particular option, they can easily be extended to other option pricing problems. The methods are based on the fitted finite volume method for spatial discretization [18], an implicit-explicit time stepping method and Crank-Nicolson time discretization scheme, coupled with FFT for the evaluation of the integral term. The Crank-Nicolson method results in a dense system matrix. To avoid the inversion of the dense matrix, we develop an iterative algorithm to solve the resulting system, based on a regular operator splitting. We prove that both of the numerical methods are unconditionally stable and their system matrices are both M -matrices. Numerical experiments are performed using Merton's model [14] and Kou's model [12]. Numerical results show that the methods are of 1st- and 2nd-order accuracy, respectively, and are robust.

The paper is organized as follows. In the next section, the mathematical model for pricing options with jump diffusion processes is presented. In Section 3, the fitted finite volume method is developed for the equation. A full discretization is proposed in Section 4 in which a stability and convergence theory for the method is also established. Also in this section, an algorithm for the numerical solution of the discretized system is proposed. Finally, in Section 5 we present some numerical results to demonstrate the convergence rates and robustness of the numerical schemes.

2. The pricing model

Let S denote the price of an asset and assume its movement follows the jump diffusion dynamics described by follow the following stochastic differential equation

$$(1) \quad \frac{dS}{S} = (\nu - \lambda\kappa) dt + \sigma dZ + (\eta - 1) dq,$$

where dZ is an increment of the standard Gauss-Wiener process and dq is the independent Poisson process with a deterministic jump intensity λ . Also in (1), σ is the volatility, ν is the drift rate; and $\eta - 1$ is an impulse function producing a jump from S to $S\eta$, and $\kappa = E(\eta - 1)$, where $E(\cdot)$ denotes the expectation operator.

Let $V(S, t)$ denote the value of a European contingent claim with striking price K on the underlying asset S and time t . By a standard argument (cf., for example, [21]), it is easy to show that $V(S, \tau)$ satisfies the following backward partial integral

differential equation (PIDE):

$$(2) \quad V_\tau = \frac{1}{2}\sigma^2 S^2 V_{SS} + (r - \lambda\kappa) V_S - (r + \lambda) V + \lambda \int_0^\infty V(S\eta)g(\eta)d\eta,$$

for $(S, \tau) \in [0, +\infty) \times [0, T]$, where r is the risk free interest rate, T is the maturity date, $\tau = T - t$, and $g(\eta)$ is the probability density function of the jump amplitude η satisfying $\int_0^\infty g(\eta)d\eta = 1$. In this paper, we consider two specific models of $g(\cdot)$: Merton's model and Kou's model.

In Merton's model, $g(\eta)$ is given by the log-normal density:

$$g(\eta) = \frac{1}{\sqrt{2\pi}\sigma_J\eta} \exp\left(-\frac{(\ln \eta - \mu)^2}{2\sigma_J^2}\right).$$

In this case, $\kappa = E(\eta - 1) = \exp(\mu + \sigma_J^2/2) - 1$, where μ and σ_J determine the mean and variance of the jumps in return.

In Kou's model, $g(\eta)$ is the following log-double-exponential density:

$$g(\eta) = p\eta_1 \exp(-\eta_1\eta)\mathcal{H}(\eta) + q\eta_2 \exp(\eta_2\eta)\mathcal{H}(-\eta),$$

where $\eta_1 > 1$, $\eta_2, p, q > 0$, $p + q = 1$, and $\mathcal{H}(\eta)$ is the Heaviside function. It can be shown that, in this case, $\kappa = E(\eta - 1) = \frac{p\eta_1}{\eta_1 - 1} + \frac{q\eta_2}{\eta_2 + 1} - 1$.

There are various types of boundary and initial conditions depending on the types of the contingent contracts. In the case of a call option, they are given by

$$(3) \quad \begin{aligned} V(0, \tau) &= 0, & S &\rightarrow 0, \\ V(\infty, \tau) &= S - Ke^{-r\tau}, & S &\rightarrow +\infty, \\ V(S, \tau = 0) &= V^*(S) = \max(S - K, 0), \end{aligned}$$

where V^* is the payoff function of the option. For a put option, we have

$$(4) \quad \begin{aligned} V(0, \tau) &= Ke^{-r\tau}, & S &\rightarrow 0, \\ V(\infty, \tau) &= 0, & S &\rightarrow +\infty \\ V(S, \tau = 0) &= V^*(S) = \max(K - S, 0). \end{aligned}$$

Other types of boundary conditions and payoff function V^* can also be imposed.

Introducing the logarithmic price $x = \ln(S)$, the pricing equation (2) is transformed as

$$(5) \quad v_\tau = \frac{1}{2}\sigma^2 v_{xx} + (r - \lambda\kappa) v_x - (r + \lambda)v + \lambda \int_{-\infty}^{+\infty} v(x + y)f(y)dy$$

for $(x, \tau) \in (-\infty, +\infty) \times [0, T]$, where

$$(6) \quad v(x, \tau) = V(e^x, \tau), \quad y = e^\eta, \quad f(y) = g(e^\eta)e^\eta.$$

The boundary and initial conditions under this transformation are

$$(7) \quad \begin{aligned} v(x, 0) &= v^*(x) = V^*(e^x), \\ v(-\infty, \tau) &= V(0, \tau), \\ v(+\infty, \tau) &= V(+\infty, \tau). \end{aligned}$$

3. The fitted finite volume method

In this section, we construct a fitted finite volume method for (5), based on the work in [16]. Since (5) is defined on the whole real line \mathbb{R} , we first need to restrict it to a finite region $I = (-x^*, x^*)$ for $x^* > 0$. It is obvious that for Merton's and Kou's models the probability density functions $g(x)$ decay exponentially as $x \rightarrow \pm\infty$. In fact, it is easy to check that the problem (5)–(7) satisfies all the

conditions required by Propositions 4.1 and 4.2 of [6]. Hence, by these propositions the following uniform truncation estimate can be established

$$|v(x, \tau) - v_I(x, \tau)| < \delta, \text{ as } x^* \rightarrow \infty$$

for a given tolerance $\delta > 0$, where $v_I(x, \tau)$ is the solution to the truncated problem (8)–(10). In other words, as x^* grows to infinity, the solution to the truncated problem converges to that of the original problem. Thus, in this paper we choose x^* is sufficiently large to ensure the truncation error is negligible.

Let

$$Q(x) = \int_I v(x+y)f(y)dy.$$

(5) can be then expressed as

$$(8) \quad v_\tau = \frac{1}{2}\sigma^2 S^2 v_{xx} + \left(r - \lambda\kappa - \frac{\sigma^2}{2}\right)v_x - (r + \lambda)v + \lambda Q(x),$$

with the boundary conditions

$$(9) \quad \begin{aligned} v(+x^*, \tau) &= e^{x^*} - Ke^{-r\tau}, & v(-x^*, \tau) &= 0, & \text{for a call,} \\ v(-x^*, \tau) &= Ke^{-r\tau} - e^{-x^*}, & v(+x^*, \tau) &= 0, & \text{for a put,} \end{aligned}$$

and the initial condition

$$(10) \quad v(x, 0) = v^*(x) = V^*(e^x).$$

Since x^* is sufficiently large, it is reasonable that $v(x, \tau)$ is replaced by the payoff function $v^*(x)$ over $\mathbb{R} \setminus I$. Now, the localized problem can be solved by the fitted finite volume method.

To discuss the fitted finite volume method, we first transform (8) in to the following form:

$$(11) \quad v_\tau = \frac{\partial}{\partial x} \left(a \frac{\partial v}{\partial x} + bv \right) - cv + \lambda Q(x),$$

where

$$(12) \quad a = \sigma^2/2, \quad b = r - \lambda\kappa - \sigma^2/2, \quad c = r + \lambda.$$

Now, we define two space partitions of I . Let $I = (-x^*, x^*)$ be divided into N sub-intervals

$$I_i = (x_i, x_{i+1}), \quad i = 1, \dots, N,$$

where, for $i = 1, 2, \dots, N+1$, $x_i = -x^* + (i-1)h$ with $h = 2x^*/N$. Setting $x_0 = x_1$ and $x_{N+2} = x_{N+1}$, we define another mesh of I as follows. For each $i = 1, 2, \dots, N+1$, let $x_{i-1/2} = (x_{i-1} + x_i)/2$ and $x_{i+1/2} = (x_i + x_{i+1})/2$. These intervals $J_i = (x_{i-1/2}, x_{i+1/2})$ form a second partition of I .

For each $i = 2, \dots, N$, integrating (11) over J_i , we have

$$(13) \quad \int_{J_i} v_\tau dx = \left(a \frac{\partial v}{\partial x} + bv \right) \Big|_{x_{i-1/2}}^{x_{i+1/2}} - \int_{J_i} cv dx + \lambda \int_{J_i} Q(x) dx.$$

Applying the mid-point quadrature rule to all the terms in (13) except the first on the right hand side, we obtain

$$(14) \quad \frac{\partial v_i}{\partial \tau} l_i = \rho(v)|_{x_{i+1/2}} - \rho(v)|_{x_{i-1/2}} - cl_i v_i + \lambda l_i Q(x_i)$$

for $i = 2, \dots, N$, where $l_i = x_{i+1/2} - x_{i-1/2} = h$ is the length of interval J_i , v_i denotes the nodal approximation to $v(x_i, t)$ to be determined and $\rho(v)$ is the flux associated with v defined by

$$\rho(v) := av' + bv.$$

We now need to derive approximations to the continuous flux $\rho(v)$ defined above at the mid-point, $x_{i+1/2}$, of the interval I_i for all $i = 1, \dots, N$. Classically, we may use conventional finite difference schemes which normally yields a piecewise linear approximation to the potential function, v . However, when the magnitude of a is very smaller than that of b , the v may varies very rapidly in a small subregion of the domain, which called a layer. In this case, a piecewise linear approximation to v normally fails to capture the layer. A better approach is to approximate the flux be a constant, which normally yields an exponential approximation to v . To achieve this, let us consider the following two-point boundary value problem:

$$(15) \quad \begin{aligned} (av' + bv)' &= 0, & x &\in I_i, \\ v(x_i) &= v_i, & v(x_{i+1}) &= v_{i+1}. \end{aligned}$$

Solving this equation analytically, we obtain

$$(16) \quad \rho_i(v) = \frac{a}{h} B\left(-\frac{bh}{a}\right) v_{i+1} - \frac{a}{h} B\left(\frac{bh}{a}\right) v_i,$$

where $B(x)$ is the Bernoulli function defined by

$$B(x) = \begin{cases} \frac{x}{e^x - 1}, & x \neq 0, \\ 1, & x = 0. \end{cases}$$

It is easy to see that

$$(17) \quad B(x) > 0, \quad \forall x \in \mathbb{R}.$$

Using $\rho_i(v)$, we define a global piecewise constant approximation to $\rho(v)$ by $\rho_h(v)$ satisfying

$$\rho_h(v) = \rho_i(v), \quad \text{if } x \in I_i$$

for $i = 1, \dots, N$. We comment that it is to see that the solution of (15) also defines a piecewise exponential approximation to the solution of (8) on I_i .

Substituting (16) into (14) and approximating the integral $Q(x_i)$ by the mid-point quadrature rule, we have

$$(18) \quad \begin{aligned} \frac{\partial v_i}{\partial \tau} l_i &= \frac{a}{h} B\left(\frac{bh}{a}\right) v_{i-1} - \frac{a}{h} \{B\left(-\frac{bh}{a}\right) + B\left(\frac{bh}{a}\right)\} v_i + \frac{a}{h} B\left(-\frac{bh}{a}\right) v_{i+1} \\ &\quad - c l_i v_i + \lambda l_i h \sum_j v_{i+j} f_j, \end{aligned}$$

for $i = 2, \dots, N$, where $f_j = f(x_j)$. Clearly, this mid-point quadrature rule has the following estimate

$$(19) \quad Q(x_i) = \int_I v(x_i + y) f(y) dy \simeq h \sum_j v_{i+j} f_j + \mathcal{O}(h^2).$$

4. Time discretization

The fitted finite volume method in the previous section yields a linear ordinary differential equation system (18). In this section we present the θ -scheme for the time discretization of (18)

$$(20) \quad \begin{aligned} \frac{v_i^{n+1} - v_i^n}{\Delta \tau} &= \theta \alpha_i v_{i-1}^{n+1} + \theta \beta_i v_{i+1}^{n+1} - \theta (\alpha_i + \beta_i + c) v_i^n + (1 - \theta) \alpha_i v_{i-1}^n + (1 - \theta) \beta_i v_{i+1}^n \\ &\quad - (1 - \theta) (\alpha_i + \beta_i + c) v_i^n + \theta_J \lambda h \sum_{j=1-i}^{N+1-i} v_{i+j}^{n+1} f_j + (1 - \theta_J) \lambda h \sum_{j=1-i}^{N+1-i} v_{i+j}^n f_j, \end{aligned}$$

for $i = 2, \dots, N$ and $n = 1, 2, \dots, L$, where

$$(21) \quad \begin{aligned} \alpha_i &= \frac{a}{l_i h} B\left(\frac{bh}{a}\right), \\ \beta_i &= \frac{a}{l_i h} B\left(-\frac{bh}{a}\right), \end{aligned}$$

and $0 \leq \theta, \theta_J \leq 1$. Note that v_1^n and v_{N+1}^n for all admissible n are determined by the boundary conditions in (9) and v_i^0 is determined by the initial condition in (10). In (20), $\theta = \theta_J = 0$, $\theta = \theta_J = 1/2$ and $\theta = \theta_J = 1$ correspond to the usual explicit, Crank-Nicolson and full implicit scheme. In this paper, we present two schemes: an implicit-explicit scheme ($\theta = 1, \theta_J = 0$) and Crank-Nicolson scheme ($\theta = \theta_J = 1/2$). For the implicit-explicit scheme, we show that it is unconditional stable. An iterative method is developed for solving the system resulting from the Crank-Nicolson scheme. Also, a mild convergence result of this iterative method will be established.

4.1. Implicit-explicit scheme. Clearly, the integral term in (18) results in a dense matrix. A full implicit scheme requires the inversion of the density matrix, which is computationally expensive. To avoid this inversion, an implicit-explicit scheme is proposed by several authors in [23]. The idea behind the implicit-explicit scheme is to use a full implicit method for the derivative terms, and use an explicit method for the jump integral term.

For a positive integer L , let the time interval $(0, T)$ be partitioned into a uniform mesh with mesh points $\tau_n = n\Delta\tau$ for $n = 0, 1, \dots, L$, where $\Delta\tau = T/L$. Let v_i^n denote the approximation of $v(x_i, \tau_n)$ for $i = 1, \dots, N+1, n = 1, \dots, L$. Then, the implicit-explicit scheme for (18) can be obtained by setting $\theta = 1, \theta_J = 0$ in (20), i.e.

$$(22) \quad v_i^{n+1} [1 + \Delta\tau(\alpha_i + \beta_i + c)] - \Delta\tau\alpha_i v_{i-1}^{n+1} - \Delta\tau\beta_i v_{i+1}^{n+1} = v_i^n + \Delta\tau\lambda h \sum_j v_{i+j}^n f_j$$

for $i = 2, \dots, N$ and $n = 1, 2, \dots, L$.

For the implicit-explicit scheme (22), we have the following stability result.

Theorem 4.1. *The implicit-explicit scheme (22) is unconditionally stable, provided that $r, \lambda \geq 0$.*

Proof. From (12),(17) and (21), it is obvious that

$$(23) \quad \alpha_i \geq 0, \quad \beta_i \geq 0, \quad 1 + (\alpha_i + \beta_i + c) \Delta\tau \geq 0,$$

provided that $r, \lambda \geq 0$. On the other hand, since

$$\int_{-\infty}^{+\infty} f(y) dy = \int_0^{\infty} g(\eta) d\eta = 1, \quad f(y) = g(e^y) e^y \geq 0,$$

it follows from (19) that

$$(24) \quad \int_I f(y) dy \simeq h \sum_j f_j \leq 1 + \mathcal{O}(h^2), \quad f_j \geq 0.$$

Let $v^n = (v_1^n, \dots, v_{N+1}^n)^\top$ be the solution to (22). For any $n = 0, 1, \dots, L$, let $E^n = (E_1^n, \dots, E_{N+1}^n)^\top$ denote the perturbation in the n th time step with $E_1^n = E_{N+1}^n = 0$ due to the Dirichlet boundary conditions. Then, from (22) we have that $\{E^n\}_0^L$ satisfies the following equation for the perturbation propagation:

$$(25) \quad E_i^{n+1} [1 + \Delta\tau(\alpha_i + \beta_i + c)] - \Delta\tau\alpha_i E_{i-1}^{n+1} - \Delta\tau\beta_i E_{i+1}^{n+1} = E_i^n + \Delta\tau\lambda h \sum_j E_{i+j}^n f_j.$$

Define a discrete maximum norm by

$$\|E^n\|_\infty = \max_i |E_i^n|.$$

Then, from (25) and (24) we have

$$\begin{aligned}
(26) \quad & \left| E_i^{n+1} \right| [1 + \Delta\tau (\alpha_i + \beta_i + c)] \\
& \leq \|E^n\|_\infty + \Delta\tau \lambda h \sum_j f_j \|E^n\|_\infty + \Delta\tau \alpha_i |E_{i-1}^{n+1}| + \Delta\tau \beta_i |E_{i+1}^{n+1}| \\
& \leq \|E^n\|_\infty + \Delta\tau \lambda [1 + \mathcal{O}(h^2)] \|E^n\|_\infty + (\Delta\tau \alpha_i + \Delta\tau \beta_i) \|E^{n+1}\|_\infty \\
& = [1 + \Delta\tau \lambda + \Delta\tau \lambda \mathcal{O}(h^2)] \|E^n\|_\infty + (\Delta\tau \alpha_i + \Delta\tau \beta_i) \|E^{n+1}\|_\infty
\end{aligned}$$

for all $i = 1, 2, \dots, N+1$ and $n = 1, 2, \dots, L-1$. This implies

$$\|E^{n+1}\|_\infty (1 + \Delta\tau c) \leq [1 + \Delta\tau \lambda + \Delta\tau \lambda \mathcal{O}(h^2)] \|E^n\|_\infty.$$

Since $c = r + \lambda$, it follows from the above that, for all $n = 1, 2, \dots, L-1$,

$$\begin{aligned}
\|E^{n+1}\|_\infty & \leq \|E^n\|_\infty \frac{1 + \Delta\tau \lambda + \Delta\tau \lambda \mathcal{O}(h^2)}{1 + \Delta\tau (r + \lambda)} = \|E^n\|_\infty \left[1 + \frac{\Delta\tau \lambda \mathcal{O}(h^2) - r \Delta\tau}{1 + \Delta\tau (r + \lambda)} \right] \\
& \leq \|E^0\|_\infty \left[1 + \frac{\Delta\tau \lambda \mathcal{O}(h^2) - r \Delta\tau}{1 + \Delta\tau (r + \lambda)} \right]^n \leq \|E^0\|_\infty \left[1 + \frac{\frac{T}{L} \lambda \mathcal{O}(h^2) - \frac{T}{L} r}{1 + \frac{T}{L} (r + \lambda)} \right]^L \\
& \leq \|E^0\|_\infty \left[1 + \frac{\lambda \mathcal{O}(h^2) - r}{L/T + (r + \lambda)} \right]^L \leq \|E^0\|_\infty \left[1 + \frac{C}{L/T} \right]^L \\
& \leq \|E^0\|_\infty e^{CT}
\end{aligned}$$

for a constant C , independent of h and $\Delta\tau$, since $r, \lambda \geq 0$. This implies that the scheme (22) is stable in time for any choices of h and $\Delta\tau$. \square

Remark 4.1. We comment that when h is sufficiently small and $r > 0$, it is easy to derive from the last inequality in the proof of Theorem 4.1 that

$$\|E^{n+1}\|_\infty \leq \|E^n\|_\infty.$$

We now write (22) in the following matrix form

$$(27) \quad [I + M] v^{n+1} = [I - D] v^n,$$

where M is a tridiagonal matrix, D is the density matrix resulting from the last term on the left-hand side of (18), and I denotes the identity matrix. For the matrix $I + M$, we have the following conclusion.

Theorem 4.2. *The matrix $I + M$ is an M -matrix.*

Proof. From (12), (17) and (21), we see that $\alpha_i, \beta_i, c \geq 0$. Hence $I + M$ has positive diagonals, non-positive off diagonals and is diagonally dominant. Hence $I + M$ is an M -matrix. \square

The above theorem shows that the fully discretized system (29) satisfies the discrete maximum principle and thus the above discretization is monotone. This guarantees that the discrete arbitrage inequality holds, which is an important property in option pricing theory.

4.2. Crank-Nicolson scheme. Although the implicit-explicit scheme used in the previous subsection is unconditionally stable, it is only first order accurate in $\Delta\tau$. To improve the accuracy, we apply Crank-Nicolson scheme to (18). By setting $\theta = \theta_J = 1/2$ in (20), we obtain the following Crank-Nicolson scheme

$$\begin{aligned}
(28) \quad & v_i^{n+1} \left[1 + \frac{\Delta\tau}{2} (\alpha_i + \beta_i + c) \right] - \frac{\Delta\tau}{2} \alpha_i v_{i-1}^{n+1} - \frac{\Delta\tau}{2} \beta_i v_{i+1}^{n+1} - \frac{\Delta\tau}{2} \lambda h \sum_{j=1-i}^{N+1-i} v_{i+j}^{n+1} f_j \\
& = v_i^n \left[1 - \frac{\Delta\tau}{2} (\alpha_i + \beta_i + c) \right] + \frac{\Delta\tau}{2} \alpha_i v_{i-1}^n + \frac{\Delta\tau}{2} \beta_i v_{i+1}^n + \frac{\Delta\tau}{2} \lambda h \sum_{j=1-i}^{N+1-i} v_{i+j}^n f_j,
\end{aligned}$$

or in the matrix form

$$(29) \quad \left[I + \frac{M}{2} + \frac{D}{2} \right] v^{n+1} = \left[I - \frac{M}{2} - \frac{D}{2} \right] v^n,$$

where M and D are the same as that in (27).

Theorem 4.3. *The matrix $I + \frac{M}{2} + \frac{D}{2}$ in (29) is an M -matrix when h and $\Delta\tau$ are sufficiently small.*

Proof. Note that the entries in D are of order $\mathcal{O}(h\Delta\tau)$. When h and $\Delta\tau$ are sufficiently small, we have that $I + \frac{M}{2} + \frac{D}{2}$ has positive diagonal elements, non-positive off diagonal elements, and is diagonally dominant. Therefore, it is an M matrix, and so is $I + \frac{M}{2} + \frac{D}{2}$. \square

Similar to the implicit-explicit scheme, we have the following result.

Theorem 4.4. *If $r, \lambda \geq 0$ and $\Delta\tau$ is sufficiently small, then the Crank-Nicolson scheme (28) is unconditionally stable.*

The proof of this theorem is similar to that of Theorem 4.1, and thus we omit this discussion.

Note that D arising from discretization of correlation product term is a dense matrix. Therefore, the solution of (29) is computationally expensive because of the inversion of D . To remedy this, we present an iterative method for (29). To achieve this, we use the regular splitting technique used in [22]. Let

$$A = I + \frac{M}{2} + \frac{D}{2} \quad \text{and} \quad b = \left[I - \frac{M}{2} - \frac{D}{2} \right] v^n.$$

We split A into

$$(30) \quad A = \left(I + \frac{M}{2} \right) - \left(-\frac{D}{2} \right) =: P - R.$$

Before further discussion, we first introduce the following definition.

Definition 4.1. *A splitting $A = P - R$ is said to be a regular splitting if $P^{-1} \geq 0$ and $R \geq 0$ (cf. [1]).*

Since we have proved in Theorem 4.3 that $I + \frac{M}{2}$ is an M matrix, it follows that $P^{-1} \geq 0$. Also from (28) and (29), we see that $D < 0$ and thus $R \geq 0$. Therefore, from the above definition, we see that the splitting (30) is a regular splitting. Using this splitting, we define an iterative scheme for (30) as follows:

$$(31) \quad P\hat{v}^{l+1} = R\hat{v}^l + b,$$

where

$$\hat{v}^{l+1} = (\hat{v}_1^{l+1}, \dots, \hat{v}_{N+1}^{l+1})^\top,$$

is an approximation to v^{n+1} after l iterations. Substituting (30) into (31), we finally obtain

$$(32) \quad \left[I + \frac{M}{2} \right] \hat{v}^{l+1} = -\frac{D}{2} \hat{v}^l + \left[I - \frac{M}{2} - \frac{D}{2} \right] v^n.$$

The following lemma establishes the convergence of the iterative method.

Lemma 4.1. *The iteration scheme (31) associated with the regular splitting (30) is convergent.*

Proof. From Theorem 4.3, we know that $A = I + \frac{M}{2} + \frac{D}{2}$ is an M matrix. Hence we have $A^{-1} \geq 0$. By the result in [1], we have that (31) is convergent. \square

Now, we give a brief description of the numerical implementation for the discretized equation systems (29). Note that the discretized equation systems (29) involve the products of the dense matrix D with the vectors. It is computationally expensive to evaluate this multiplication directly, because the computational cost is $\mathcal{O}(N^2)$. Here, we present a fast algorithm for the evaluation of these matrix products. This algorithm, based on Fast Fourier Transform (FFT), has a computational cost of order $\mathcal{O}(N \ln N)$. For brevity, we take the iteration scheme (32) and consider the product of R and \widehat{v}^l for each iteration step.

From (19) and (30) we see that R is a Toeplitz matrix. Applying the FFT to $R\widehat{v}^l$ will produce undesirable wrap-around pollution. To avoid this, a commonly used technique is to embed the Toeplitz matrix R into a circulant matrix C (cf. [13]). If we define

$$u^{l+1} = [\widehat{v}_1^{l+1}, \dots, \widehat{v}_{N+1}^{l+1}, \underbrace{0, \dots, 0}_N]^T,$$

then the matrix-vector product $R\widehat{v}^l$ is then realized as the first $N + 1$ entries in Cu^{l+1} .

Remark 4.2. *The first and $(N + 1)$ th entries should be set to the corresponding boundary conditions (9), since the Dirichlet boundary conditions are used in the first and $(N + 1)$ th nodes.*

Following the ideas stated above, we can compute the product $R\widehat{v}^l$ in the following two FFT operations. Let $FFT(w)$ denote the FFT of w and define the vector

$$F = (f_0, f_1, \dots, f_N, f_{-N}, f_{1-N}, \dots, f_{-1}),$$

which generates the row vectors of C by permutation. First, we compute $FFT(F)$ and $FFT(u)$. Then, we compute the inverse FFT of the product of $FFT(f)$ and $FFT(u)$.

Summarizing the numerical implementation details for the system (29), we have the numerical algorithm as follow:

Algorithm 4.1.

- 1: Let $n = 0$.
- 2: Compute $FFT(F)$.
- 3: Set $l = 0$ and $\widehat{v}^0 = v^n$.
- 4: Compute $FFT(u^l)$.
- 5: Compute the inverse FFT of the product of $FFT(f)$ and $FFT(u)$ which gives $R\widehat{v}^l$.
- 6: Solve

$$P\widehat{v}^{l+1} = R\widehat{v}^l + b.$$

- 7: If $\max_i \frac{|\widehat{v}_i^{l+1} - \widehat{v}_i^l|}{\max(1, |\widehat{v}_i^{l+1}|)}$ < tolerance, then stop. Otherwise, let $l = l + 1$ and go to Step 4.
- 8: Set $v^{n+1} = \widehat{v}^{l+1}$ and $n = n + 1$; go to Step 3.

5. Numerical experiments

In this section, we present some numerical results to illustrate the performance and convergence of the implicit-explicit scheme and Crank-Nicolson scheme. Two models, those of Merton and Kou with parameter values of of practical significance, are chosen as our test examples. In the numerical experiments, we investigate the convergence property of the iterative method for solving the discrete algebraic equations at each time step and rates of convergence of the discretization schemes.

Parameter values					
r	0.00	μ	0.00	K	1.00
σ	0.20	σ_J	0.50	T	1 and 2
		λ	0.10		

TABLE 1. Data used to value European options under Merton’s model

Parameter values					
r	0.00	η_2	3.0		
σ	0.20	η_1	2.0	K	1.0
λ	0.20	p	0.5	T	0.2
μ	0.00	q	0.5		

TABLE 2. Data used to value European options under Kou’s model

Because of the non-smoothness of the payoff function, the usual second order convergence rate of the Crank-Nicolson scheme may not be sustained. To remedy this, we use the technique proposed in [17].

For Merton’s and Kou’s models, analytic solutions are available. Thus, to verify the accuracy of our numerical schemes, we simply compare our numerical solutions with the exact ones. The parameters used in Merton’s and Kou’s models are listed respectively in Table 1 and Table 2.

For Merton’s model with the parameters in Table 1, we choose $x^* = 4$. The coarsest grid is defined as $h = 2x^*/2^6$ and $\Delta\tau = 0.2$. Note that the number of sub-intervals N has to be a multiple of 2 because of the FFT algorithm.

For Kou’s model with the parameters in Table 2, we set $x^* = 6$. The coarsest grid is defined as $h = 2x^*/2^6$ and $\Delta\tau = 0.02$.

To determine the numerical rates of convergence, we choose a sequence of meshes by successively halving the mesh parameters. At $\tau = 0$, we compute the following ratios of the numerical solutions of the consecutive meshes :

$$(33) \quad \text{Ratio}(\|\cdot\|_\infty) = \frac{\|V_{\Delta\tau}^h - V\|_\infty}{\|V_{\Delta\tau/2}^{h/2} - V\|_\infty}$$

in the solution domain, where V_α^β denotes the computed solution on the mesh with spatial mesh α and time mesh size β , V is the exact solution,

$$\|V_{\Delta\tau}^h - V\|_\infty := \max_{1 \leq i \leq N-1} |V_i^0 - V(S_i, \tau = 0)|.$$

The numerical order of convergence is then defined by

$$\text{Rate} = \log_2 \text{Ratio}.$$

All the numerical experiments were carried out on a dual 1.86GHz Pentium IV PC.

Example 5.1. *Numerical tests for the fitted finite volume method combined with the implicit-explicit scheme*

The numerical results for Merton’s and Kou’s models are listed respectively in Tables 3 and 4. From these tables we see that the computed rates of convergence are at least of first-order, which coincides with the theoretical first-order convergence rate of the backward Euler time discretization used in the implicit-explicit scheme. Note that the rate of convergence of the spatial discretization is of a 2nd-order, as can be seen below. However, since the time discretization is only first-order accurate, we only get the first-order numerical convergent rates in this case.

x -steps	$\Delta\tau$	$T = 1$			$T = 2$				
		$V(K, 0)$	$\ \cdot\ _\infty$	Ratio	CPU	$V(K, 0)$	$\ \cdot\ _\infty$	Ratio	CPU
64	1/5	0.0868691	0.2519		0.01s	0.1316979	0.3103		0.01s
128	1/10	0.0917697	0.1166	2.2	0.01s	0.1350245	0.1481	2.1	0.01s
256	1/20	0.0931992	0.0559	2.1	0.02s	0.1361496	0.0714	2.1	0.02s
512	1/40	0.0937251	0.0273	2.0	0.04s	0.1365939	0.0350	2.0	0.07s
1024	1/80	0.0939444	0.0134	2.0	0.15s	0.1367876	0.0173	2.0	0.27s
2048	1/160	0.0940434	0.0067	2.0	0.59s	0.1368774	0.0086	2.0	1.17s
4096	1/320	0.0940903	0.0033	2.0	2.24s	0.1369206	0.0045	2.0	4.53s
8192	1/640	0.0941131	0.0017	1.9	9.19s				
Exact solution		0.09413553				0.13696311			

TABLE 3. Results for European call options under Merton's model using the fitted finite volume method combined with the implicit-explicit scheme, data as in Table 1. $\|\cdot\|_\infty$ stands for $\|V_{\Delta\tau}^h - V\|_\infty$. CPU represents the CPU time

x -steps	$\Delta\tau$	$V(K, 0)$	$\ \cdot\ _\infty$	Ratio	CPU
64	0.2/10	0.0264343	1.2696		0.01s
128	0.2/20	0.0364626	0.8612	1.5	0.01s
256	0.2/40	0.0412580	0.3758	2.3	0.02s
512	0.2/80	0.0422908	0.1668	2.3	0.07s
1024	0.2/160	0.0425455	0.0775	2.2	0.27s
2048	0.2/320	0.0426155	0.0373	2.1	1.09s
4096	0.2/640	0.0426360	0.0187	2.0	4.57s
Exact solution		0.0426761			

TABLE 4. Results for European call options under Kou's model using the fitted finite volume method combined with the implicit-explicit scheme, data as in Table 2. $\|\cdot\|_\infty$ stands for $\|V_{\Delta\tau}^h - V\|_\infty$. CPU represents the CPU time

Example 5.2. *Numerical tests for the fitted finite volume method combined with the Crank-Nicolson scheme*

The numerical experiments require the use of Algorithm 1 and we set the *tolerance* in Algorithm 4.1 to 10^{-8} . Tables 5 and 6 contain the numerical results for Merton's and Kou's models, respectively.

From Table 5 and Table 6, quadratic convergence rate of the Crank-Nicolson scheme is clearly observed. Compared with Tables 3 and 4, the Crank-Nicolson scheme is more accurate. Both the Crank-Nicolson scheme and the implicit-explicit scheme converge to the same solution. From Table 5 and Table 6 we see that the computed rates of convergence approximate to 2, indicating that the discretization error of the scheme is of order $\mathcal{O}(h^2 + \Delta\tau^2)$. From the tables we also see that the average number of iterations per time step is 1 to 2. Certainly, the number of iterations depends on the convergence tolerance. For a convergence tolerance of 10^{-8} , the fitted finite volume method combined with the Crank-Nicolson scheme is very efficient.

To conclude this section, we plot, in Figure 1, the value and their first and second derivatives (delta and gamma respectively) at the last time step of the European option with a particular choice of parameter set. From Figure 1 we can see that the option value, delta and gamma are qualitatively very good and contain

x -steps	$\Delta\tau$	$T = 1$					$T = 2$				
		$V(K, 0)$	$\ \cdot\ _\infty$	Ratio	Itns	CPU	$V(K, 0)$	$\ \cdot\ _\infty$	Ratio	Itns	CPU
64	1/5	0.0890816	0.2272		9	0.01s	0.1339778	0.2565		19	0.01s
128	1/10	0.0929685	0.1033	2.2	19	0.02s	0.1362362	0.1115	2.3	39	0.01s
256	1/20	0.0938467	0.0397	2.6	39	0.05s	0.1367818	0.0413	2.7	79	0.02s
512	1/40	0.0940633	0.0128	3.1	41	0.12s	0.1369174	0.0129	3.2	81	0.07s
1024	1/80	0.0941174	0.0036	3.6	81	0.50s	0.1369514	0.0039	3.3	161	0.27s
2048	1/160	0.0941310	0.0010	3.3	161	2.21s	0.1369598	0.0011	3.5	321	1.17s
4096	1/320	0.0941343	0.0003	3.0	321	9.39s	0.1369620	0.0003	3.7	641	4.53s
8192	1/640	0.0941352	0.0001		641	39.4s					
Exact solution							0.0941355				
							0.1369631				

TABLE 5. Results for European call options under Merton’s model using the fitted finite volume method combined with the implicit-explicit scheme, data as in Table 1. $\|\cdot\|_\infty$ stands for $\|V_{\Delta\tau}^h - V\|_\infty$. CPU is the CPU time. Itns is the total number of iterations required in Algorithm 4.1, for all time steps. Rannacher smoothing is used. $tolerance = 10^{-8}$

x -steps	$\Delta\tau$	$V(K, 0)$	$\ \cdot\ _\infty$	Ratio	Itns	CPU
64	0.2/10	0.0266393	1.0786		19	0.01s
128	0.2/20	0.0367510	0.5136	2.1	21	0.02s
256	0.2/40	0.0413999	0.2140	2.4	41	0.06s
512	0.2/80	0.0423562	0.0649	3.3	81	0.29s
1024	0.2/160	0.0425780	0.0167	3.9	161	1.04s
2048	0.2/320	0.0426315	0.0046	3.6	321	4.44s
4096	0.2/640	0.0426442	0.0014	3.3	641	17.6s
Exact solution		0.0426761				

TABLE 6. Results for European call options under Kou’s model using the fitted finite volume method combined with the implicit-explicit scheme, data as in Table 1. $\|\cdot\|_\infty$ stands for $\|V_{\Delta\tau}^h - V\|_\infty$. CPU is the CPU time. Itns is the total number of iterations required in Algorithm 4.1, for all time steps. Rannacher smoothing is used. $tolerance = 10^{-8}$

no oscillations. It shows that the fitted finite volume method combined with the Crank-Nicolson scheme is robust.

6. Conclusion

In this work we developed an exponentially fitted finite volume method for the spatial discretization of the PIDE governing European option prices under the jump diffusion process. The method is coupled with two different time-stepping schemes. We have shown that the discretization schemes are unconditionally stable and the system matrices of the fully discretized equations are M -matrices. To handle products of the dense matrix with vectors arising from the discretization of the integral operator in the PIDE, we propose the use of FFT. One of the fully discretized systems involves the inversion of the dense matrix and we proposed an iterative method for handling this difficulty. Numerical experiments were performed using two known models to demonstrate the accuracy and efficiency of the methods. The numerical results show that the methods are stable and the rates of convergence are of respectively 1st and 2nd-orders.

Acknowledgments

The authors would like to thank one anonymous referee for the valuable comments toward the improvement of this paper. The support of the Australian Research Council is also gratefully acknowledged.

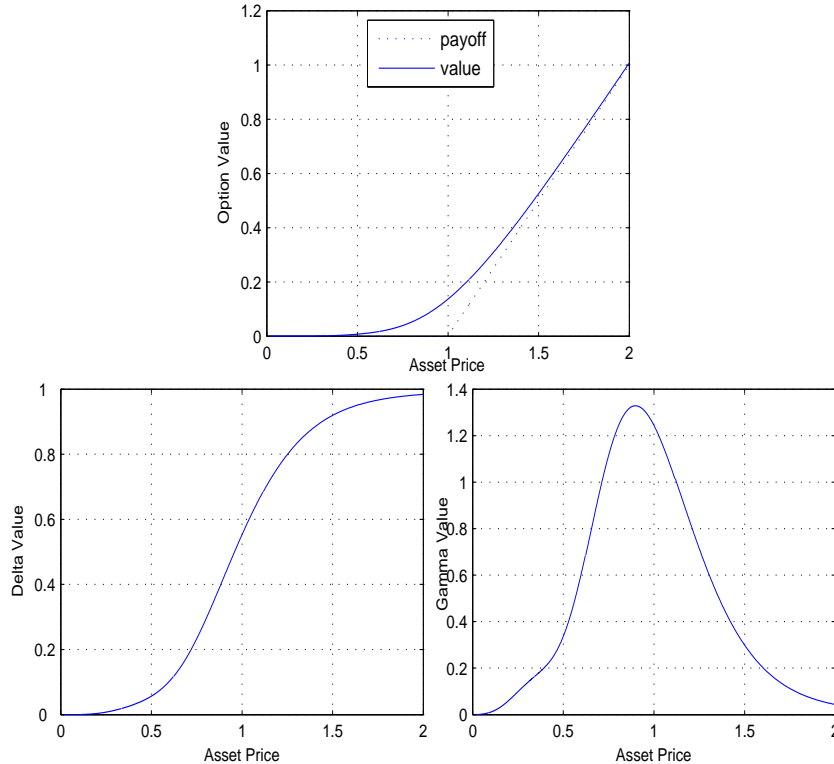


FIGURE 1. European option value, delta and Gamma at the last time step, with $r = 0.0$, $\sigma = 0.2$, $\mu = 0.0$, $\sigma_J = 0.50$, $\lambda = 0.1$, $K = 1.0$, $T = 2.0$. Rannacher smoothing is used. $tolerance = 10^{-8}$. Grid: $x\text{-steps} = 212$, $\Delta\tau = 1/640$.

References

- [1] A. Almendral and C.W. Oosterlee, Numerical valuation of options with jumps in the underlying, *Appl. Math. Comput.*, 53 (2005), 1-18.
- [2] K. Amin, Jump diffusion option valuation in discrete time, *J. Finance*, 48 (1993), 1883-1863.
- [3] A. Anderson and J. Andresen, Jump diffusion process: Volatility smile fitting and numerical methods for option pricing, *Rev. of Derivatives Res.*, 4 (2000), 231-262.
- [4] F. Black and M. Scholes, The pricing of options and corporate liabilities, *J. Political Economy*, 81 (1973), 637-659.
- [5] R. Cont and P. Tankov, *Financial Modelling with Jump Processes*, Chapman and Hall/CRC, Boca Raton, FL, 2004.
- [6] R. Cont and E. Voltchkova, A finite difference scheme for option pricing in jump diffusion and exponential Lévy models, *SIAM J. Numer. Anal.*, 43 (2005), 1596-1626.
- [7] D.J. Duffy, *Finite Difference Methods in Financial Engineering: A Partial Differential Equation Approach*, Wile Finance, West Sussex, England, 2006.
- [8] B. Dupire, Pricing with a smile, *Risk*, 7 (1994), 18-20.
- [9] S.L. Heston, A closed-form solution for options with stochastic volatility with applications to bond and currency options, *Rev. Financial Stud.*, 6 (1993), 327-343.
- [10] J. Hull, *Options, Futures, and Other Derivatives*, Prentice-Hall, Englewood Cliffs, 2005.
- [11] J. Hull and A. White, The pricing of options on assets with stochastic volatilities, *J. Finance*, 42 (1987), 281-300.
- [12] S.G. Kou, A jump-diffusion model for option pricing, *Management Sci.*, 48 (2002), 1086-1101.

- [13] C. Van Loan, Computational Frameworks for the Fast Fourier Transform, Frontiers in Applied Mathematics, vol. 10, SIAM, Philadelphia, PA, 1992.
- [14] R.C. Merton, Option pricing when underlying stock return are discontinuous, J. Financial Econ., 3 (1976), 125-144.
- [15] J.J.H. Miller and S. Wang, A new non-conforming Petrov-Galerkin method with triangular elements for a singularly perturbed advection-diffusion problem, IMA J. Numer. Anal., 14 (1994), 257-276.
- [16] J.J.H. Miller and S. Wang, An exponentially fitted finite element volume method for the numerical solution of 2D unsteady incompressible flow problems, J. Comput. Phys., 115 (1994), 56-64.
- [17] R. Rannacher, Finite element solution of diffusion problems with irregular data, Num. Math., 43 (1984), 309-327.
- [18] S. Wang, A novel fitted finite volume method for the Black-Scholes equation governing option pricing, IMA J. Numer. Anal., 24 (2004), 699-720.
- [19] G. Wang and X. Yang, The regularization method for a degenerate parabolic variational inequality arising from American option valuation, Int. J. Numer. Anal. Mod., 5 (2008), 222-238.
- [20] S. Wang, X.Q. Yang, and K.L. Teo, Power penalty method for a linear complementarity problem arising from American option valuation, J. Optim. Theory Appl., 129 (2006), 227-254.
- [21] P. Wilmott, Derivatives, Wiley, New York, 1998.
- [22] D.M. Young, Iterative Solution of Large Linear Systems, Academic Press, New York, 1971.
- [23] X.L. Zhang, Numerical analysis of American option pricing in a jump diffusion model, Math. Oper. Res., 22 (1997), 668-690.

(K. Zhang) Department of Finance, Business School, Shenzhen University, Nanshan District, Shenzhen, Guangdong, P.R.China, 518060

(S. Wang) School of Mathematics and Statistics, The University of Western Australia, 35 Stirling Hwy, Crawley, WA 6009, Australia

E-mail: mazhangkai@gmail.com and swang@maths.uwa.edu.au